Post-stack attribute analysis of the 9C seismic survey – Olds, Alberta

Vladan Simin

ABSTRACT

Seismic attribute analysis was performed on the Olds 9C-2D line. Data around two wells, one with 6% porosity and the other one with tight, bedded dolomite, on the line were compared. Quality of data varied between different component stacks with P-P, P-SV, SH-SH, and P-SH chosen for the analysis. This analysis was two-fold – comparison of attributes around the two wells and comparison of stacked sections using FXTRAN program (Schoepp and Margrave, 1996). Top of Wabamun signal strength on instantaneous amplitude display tends to dim with increased porosity but increases inside the reservoir. Instantaneous frequency tends to be more continuous in tight low porosity carbonates. Frequency spectrum analysis clearly shows reduction in frequency from P-wave to pure SH-wave sections. Converted compressional to horizontal shear section has enough coherent signal to suggest anisotropy at the zone of interest.

INTRODUCTION

Traditionally P-wave data is used to obtain as much structural and stratigraphic detail as possible and for many years this was thought to be a sufficient tool in geophysical exploration. In the last ten years elastic wave theory has finally started to find its way into the practical and business-oriented world of exploration geophysics as we started to realize the benefits of full waveform seismic.

Estimating reservoir and rock properties like lithology, porosity, fluid type and imaging with more detail through gas clouds are some of the reasons why multicomponent surveys are gaining in popularity. A nine component survey is the most complete experiment, surface seismic could offer. Nine final data volumes (three pure and six converted wave sections) offer a wealth of information, some of which are more useful than others. Due to the high costs associated with 9C acquisition and processing (Tatham and McCormack, 1991), these surveys are few and far between and will continue to be used only in difficult to interpret areas.

Amerada Hess Corporation Limited conducted a 9C-2D seismic survey in the summer of 1993. 3C vibroseis at 90m source intervals were used along with 300 3C geophones at 15m group intervals (Yang and Stewart, 1996). This line was acquired in attempt to delineate the thickness and extent of productive reservoir-quality dolomites in the Olds field (Bednar, 1995). Conventional P-P seismic data was ineffective because the reservoir dolomite is encased in anhydrite which has compressional velocities similar to those of the dolomite (Mills, 1993). This work attempts to determine if it is possible to show the separation between high porosity shoal deposits and low permeability bedded and mottled facies to the east.

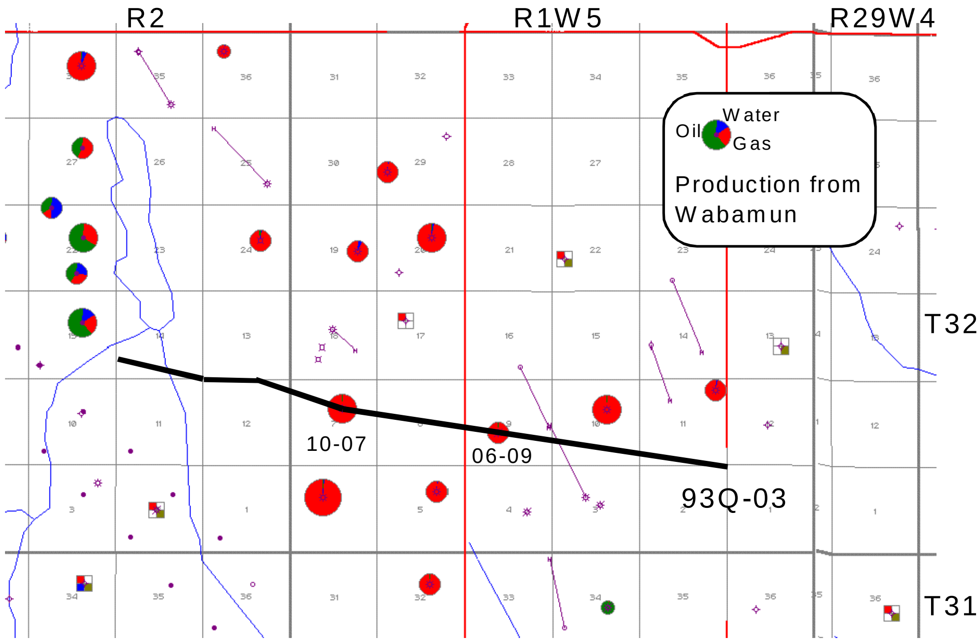

Figure 1: Olds gas field and 9C-2D seismic line

GEOLOGY

Olds Gas Field is located 65km north of Calgary, Alberta and is at the north end of a north south productive trend extending 145km. The producing formation is the Devonian Wabamun Crossfield member. This formation consists of alternating high porosity dolomite stromatoporoid shoals and low porosity bedded dolomite.

Geologic model shows that stromatoporoid facies are flanked by open marine facies to the west and bedded and mottled facies followed by Sabkha anhydrite to the east. In addition, the Crossfield member is encased in anhydrites which further complicates its detection on seismic data since dolomite exhibits similar P-wave velocities to that of anhydrites. Lack of dipole sonics in the area prevents us from predicting impedance contrasts for the S-wave velocities.

Two wells are located very close to the 9C seismic line:

- 10-7-32-1W5 encountered 6% porosity and approximately 100md permeability in the Crossfield member from 8688 to 8735 ft (Mills, 1993). This well is located 153m south of source point (SP) 581 and is a good gas producer.
- 6-9-32-1W1 encountered tight low porosity dolomite. It is located 113m south of SP 381.

The producing well seems to have penetrated the eastern flank of stromatoporoid shoal, while 6-9 was drilled into tight low permeability bedded dolomite (AHCL, 1993). In addition to intermittent stromatoporoid facies, reservoir porosity can be greatly affected by cementing of the original pore space by anhydrite or calcite seeping.

METHOD

The objective of this work is twofold. 1) Identify the zone of interest, interpret the main reflectors, tie compressional, converted and pure shear wave sections and then attempt to determine if complex trace seismic attributes can help us in mapping porous dolomite reservoir in the Olds gas field. 2) Analyze signal to noise ratio (S/N) for different components and their ability to bring additional information as compared to the conventional P-wave data.

Complex trace analysis starts with a complex number representation of the time series (after Sheriff, 1991):

$$F(t) = f(t) + jf^{*}(t) = A(t)e^{j\gamma(t)}$$

Where f(t) is the seismic trace in time, and f*(t) is the imaginary component of the complex trace - a 90 degree phase shift of f(t) using Hilbert transform (Vetrici and Stewart, 1996). Instantaneous attributes become clear when we write F(t) in a polar form:

- Instantaneous amplitude A(t) is the amplitude of the envelope (also known as reflection strength) that is proportional to the square root of the total energy. This is an effective tool for identifying rapid lateral changes in reflectivity (bright and dim spots).
- Instantaneous phase $\gamma(t) = \arctan[f^*(t)/f(t)]$ is a measure of event continuity on a seismic section (faults, onlaps, pinchouts).
- Instantaneous frequency $\omega(t) = d\,\gamma(t)/dt$ is a temporal measure of the rate of change of instantaneous phase (Yilmaz, 1987). This attribute's high variability may be related to lithology and therefore may be able to discriminate between reservoir and non-reservoir rocks.

Four component datasets were chosen for this study: P-P, pure compressional wave data, SH-SH, pure shear wave data, P-SV and P-SH (Figures 2 to 5). The P-SV has the highest S/N ratio among the converted wave datasets, and P-SH is considered for anisotropy. Main reflections around the zone of interest were identified on the P-P stack using 10-07 well log synthetics. Two-way travel times were estimated for top of Wabamun and its producing Crossfield member using depth logs, and average and interval velocities. This was followed by correlating the remaining three sections with the P-P data. Complex trace attributes were calculated for all four components and displayed with interpreted horizon tops.

Signal to noise estimates were conducted by calculating frequency spectra (Sheriff and Geldart, 1982) through FXTRAN, a MATLAB based one-dimensional fourier transform program written by Gary Margrave (Foltinek and Bland, 1996). The program allows the limits of frequency and phase lateral variations around the zone of interest to be observed.

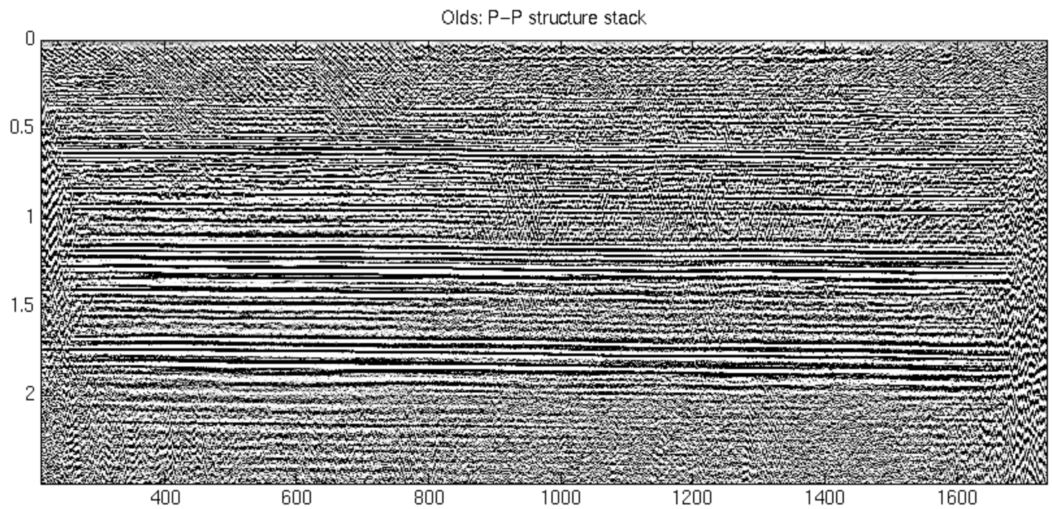

Figure 2: P-P stack

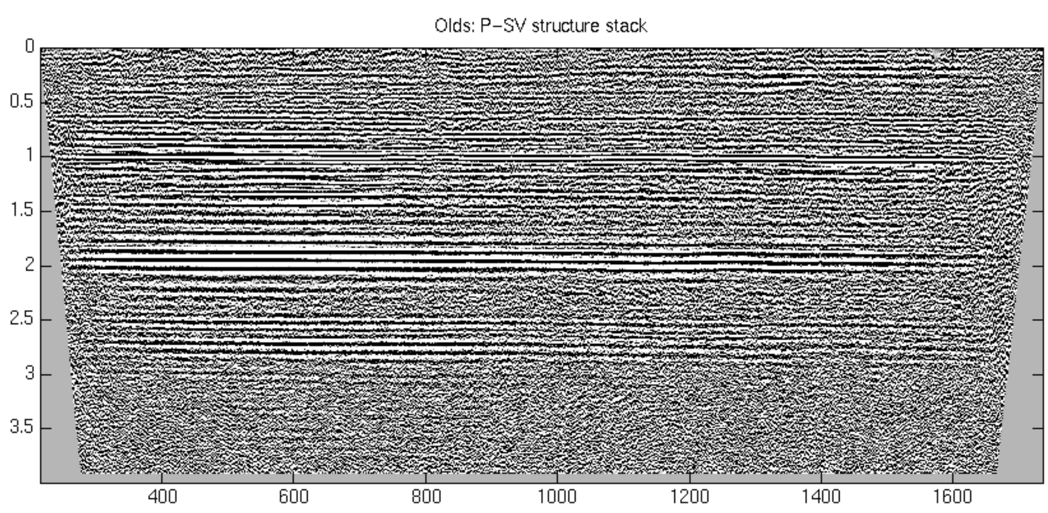

Figure 3: P-SV stack

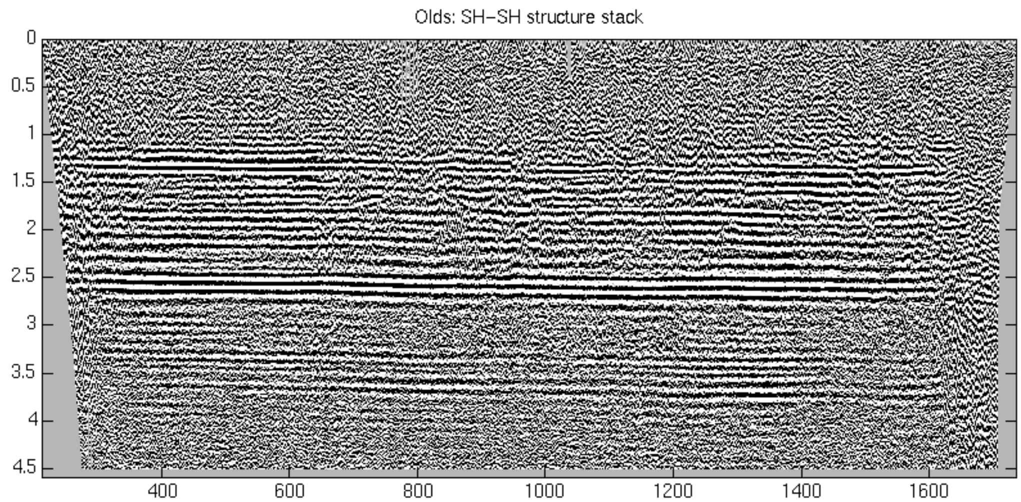

Figure 4: SH-SH stack

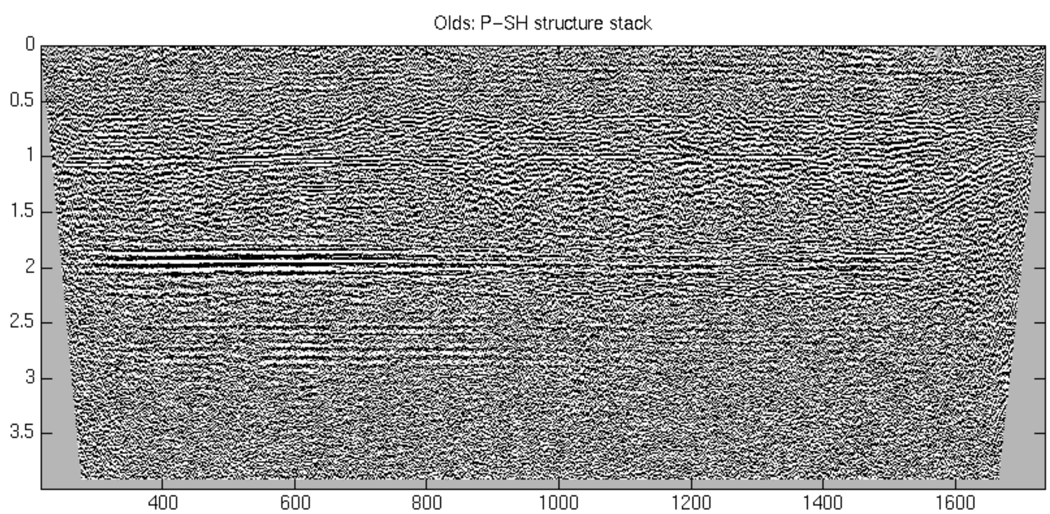

Figure 5: P-SH stack

RESULTS

Of the nine component stacked sections only SH-P does not contain coherent energy. The rest of the sections show varying degrees of coherent reflection events. A P-P section was interpreted first using 10-7 synthetic. Travel times were computed from depth, V_{ave} and V_{int} logs to confirm correlation. While the absolute two-way times were off by ~20ms, probably due to velocity dispersion of the higher frequency log tool (Stewart, et al., 1984), relative times confirmed visual correlation. The Pekisko, Banff, Wabamun and Crossfield events were identified along with two strong markers one immediately below Banff shale trough (marked UM) and the other immediately below the Crossfield member (marked LM). Wabamun and these two markers are consistent on the other component stacks. Consequently, they were picked on all stacked sections, and used to correlate shear and converted wave data with the P-P section.

Zone of interest was identified to be between Wabamun and the lower marker. Instantaneous amplitude (IA), phase (IP), and frequency (IF) sections on the representative compressional, converted, and shear wave sections (P-P, P-SV, SH-SH, and P-SH – for anisotropy consideration) were created. Data was extracted around the producing well (10-7) and the non-producing well (6-9). Some of the observations are summarized below.

P-P IA: Data around the 6-9 well exhibits stronger reflectivity at the top of Wabamun but weaker and less consistent response than 10-7 at the reservoir level (Figure 6). This could be due to tight dolomite at 6-9 producing stronger impedance contrasts.

P-SV IA: As in P-P section we see stronger response at the Wabamun/Exshaw level around the 6-9 well but inconclusive results at the Crossfield level (Figure 7).

P-P IF: Instantaneous frequency display is more continuous and smooth at 6-9 below Wabamun, suggesting more laterally consistent lithology (Figure 8).

P-SV IF: Very little difference can be seen between 10-7 and 6-9 wells and no hint of lateral inhomogeneities on either display. This could be a result of over-smoothing the data using FX deconvolution or F-K filtering in an attempt to improve S/N ratio of noisy data.

SH-SH IP: Data around both 6-9 and 10-7 show continuity at and above the reservoir level but no discernible differences between the two (Figure 9).

P-SH stacked, IA, and IP data is shown in figure 10 to illustrate relatively impressive signal strength and continuity through most of the eastern end of the line. This could suggest existence of fracture-generated anisotropy in the area. Other possible explanations of a coherent P-SH section include leaking P-SV signal onto the transverse component or a strong shear wave generation by a P-wave vibroseis truck sitting on a thick layer of unconsolidated soil.

Second part of the study involves lateral spectral analysis around the zone of interest. FXTRAN, a Matlab-based Fourier transform program was used to study frequency and phase extent of the four stacked sections. Figures 11 and 12 display P-P, P-SV, SH-SH, and P-SH average frequency spectrum and lateral extent of coherent complex phase and frequency spectra. Table 1 below summarizes the results.

P-P shows frequency range of 15-50 Hz with ~35 Hz dominant frequency and consistent phase to approximately 60 Hz. P-SV data experiences a marked drop in all three attributes, 10-20 Hz range with 17 Hz dominating and up to 28 Hz laterally consistent phase. Frequencies drop even further for an SH-SH stack. While these values have been observed in other multicomponent seismic surveys, it is interesting that frequency attributes for the P-SH stack are comparable to P-SV numbers and higher than SH-SH section which has a stronger signal. This shows that converted wave data inherently has higher power of resolution than pure shear wave.

Section	Frequency Spectra (Hz)	Phase Spectrum (Hz)	Dominant Frequency (Hz)
P-P	15 – 50	0 – 60	35
P-SV	10 – 20	0 – 28	17
SH-SH	10 – 15	0 – 15	10
P-SH	10 – 20	0 – 22	17

Table 1. Results of spectral analysis of the four stacked sections around the zone of interest interval.

CONCLUSIONS

Olds 9C-2D seismic survey yields nine stacked sections of varying quality. P-P, P-SV, SH-SH, and P-SV were chosen for our seismic attribute study as best representatives of compressional, converted, and shear waves and possible anisotropy indicators. Two wells placed close to the line provided the opportunity for direct comparison of a 9C seismic response to a producing Crossfield dolomite in well 10-7 versus a tight dolomite encountered at the same level in well 6-9. Post-stack seismic attribute analysis was carried out in hope of delineating stromatoporoid shoal facies from tight bedded and mottled facies. Both P-P and P-SV exhibit stronger reflectivity (envelope amplitude) around well 6-9 at the Wabamun level but weaker reflectivity at the Crossfield level. This could well be a result of the tighter, more competent carbonate producing a stronger response and then homogeneously continuing into the Crossfield member. Instantaneous frequency display of the P-P stack shows better continuity below Wabamun around 6-9 suggesting more consistent lithology. These indications are consistent but the degree of confidence could not justify risks involved. There is an interesting anomaly on both P-P and converted wave data around SP 522 that warrants a closer look on pre-stack CDP and CCP gathers.

P-SH data has a low S/N ratio but shows surprising coherency in the east end of the line considering that particle motion at conversion point has to change from vertical to horizontal plane. This suggests existence of azimuthal anisotropy (most likely induced by fractures in the carbonate sequence) or acquisition artifacts.

Lateral frequency and phase analysis provided a more quantitative comparison between compressional, converted, and shear sections. Loss of frequency and laterally consistent phase was evident going from P-P to P-SV to SH-SH data. However, P-SH despite lower signal quality preserved frequency and phase close to the P-SV levels. This experiment showed converted wave's advantage over pure shear data in both cost savings and quality of imaging.

FUTURE WORK

Primary goal of any further work on this dataset should be re-processing the data from scratch. Converted wave processing modules are continuously being improved upon and are more sophisticated than in 1993. Depth-variant binning, converted wave DMO and P-SV post-stack migration are some of the routines that are now available. In addition, birefringence analysis should be performed to study possible anisotropic effects. Pure shear data could be used to establish a near-surface shear velocity model. This could help us resolve receiver and shot statics in converted and pure shear data. Pre-stack AVO analysis could also improve our understanding of subtle lithological changes in the Wabamun formation.

ACKNOWLEDGMENTS

I would like to thank Dr. Rob Stewart, Mr. Colin Potter and Ms. Grace Yang for their help and insight.

REFERENCES

AHCL, 1993, Amerada Hess Corporation Limited internal geology report.

Bednar, B.J., 1995, Amerada Hess Corporation Limited internal correspondence.

Foltinek, D.S., and Bland, H.C., 1996, CREWES Software Release: CREWES Research Report, Vol. 8, Ch.31.

Mills, J., 1993, Amerada Hess Corporation Limited internal communication.

Schoepp, A.R., and Margrave, G.F., 1996, Signal band estimation of the Blackfoot 3C-3D experiment: CREWES Research Report, Vol. 8, Ch.43, p.7.

Sheriff, R.E., 1991, Encyclopedic Dictionary of Exploration Geophysics, Third Ed., SEG.

Sheriff, R.E., and Geldart, L.P., 1982, History, theory and data acquisition: Cambridge University Press.

Stewart, R.R., Huddleston, P.D., and Kan, T.K., 1984, Seismic versus sonic velocities: A vertical seismic profiling study: Geophysics, 49, 1153-1168.

Tatham, R.H., and McCormack, M.D., 1991, Multicomponent Seismology in Petroleum Exploration. Investigations in Geophysics Series Vol. 6. Society of Exploration Geophysicist.

Vetrici, G.R., and Stewart, R.R., 1996, 3-D seismic attributes: CREWES Research Report, Vol. 8.

Yang, G.Y.C., and Stewart, R.R., 1996, 9C-2D seismic data analysis: Olds, Alberta: CREWES Research Report, Vol. 8, Ch.32.

Yilmaz, O., 1987, Seismic Data Processing, Investigations in Geophysics Series Vol. 2. Society of Exploration Geophysicist.

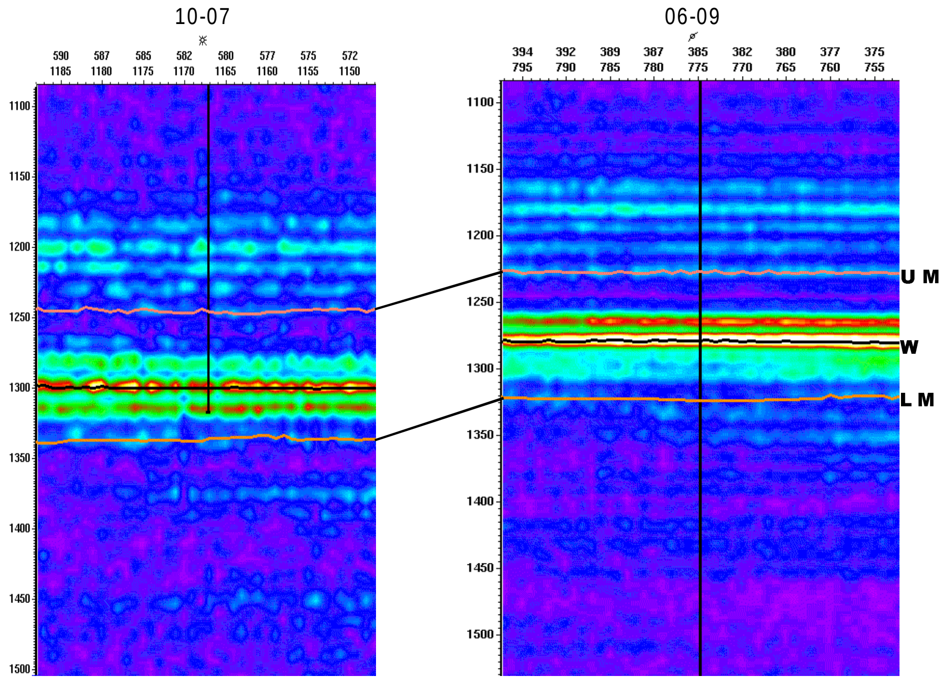

Figure 6: P-P Instantaneous amplitude

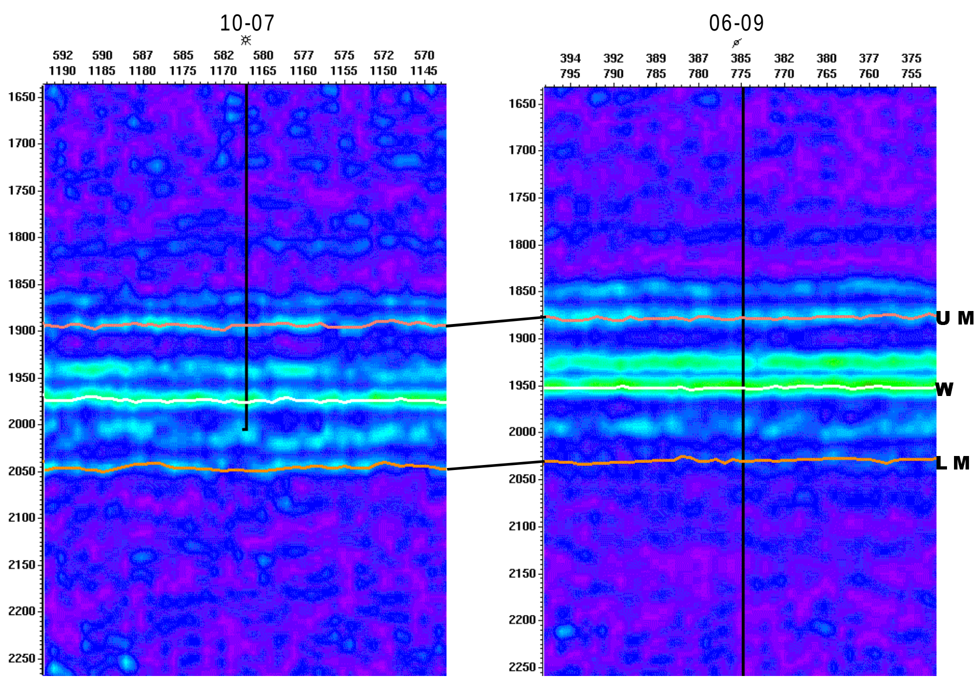

Figure 7: P-SV instantaneous amplitude

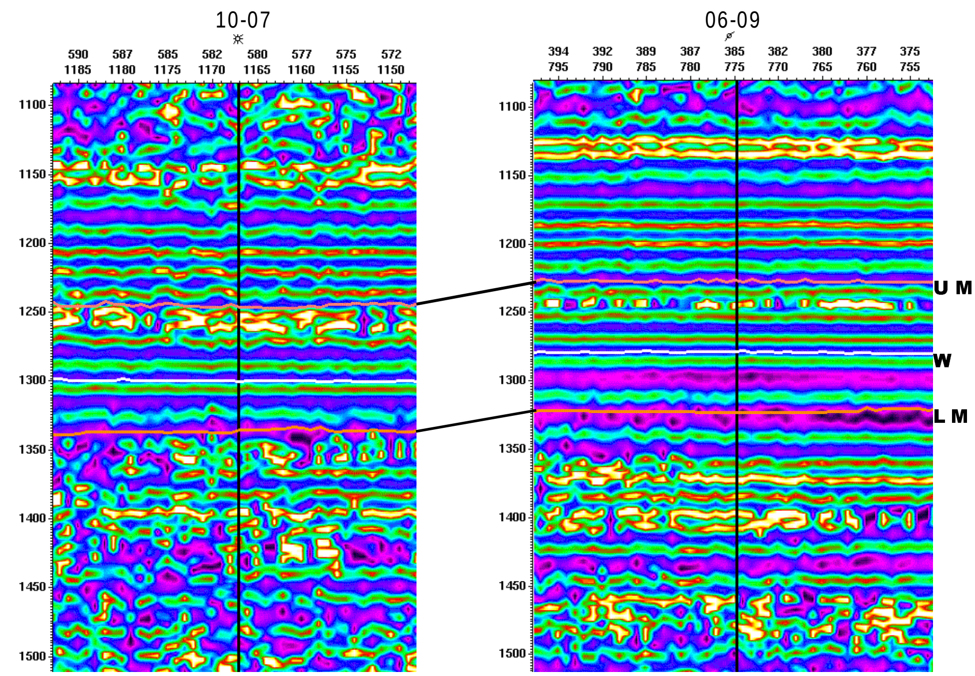

Figure 8: P-P instantaneous frequency

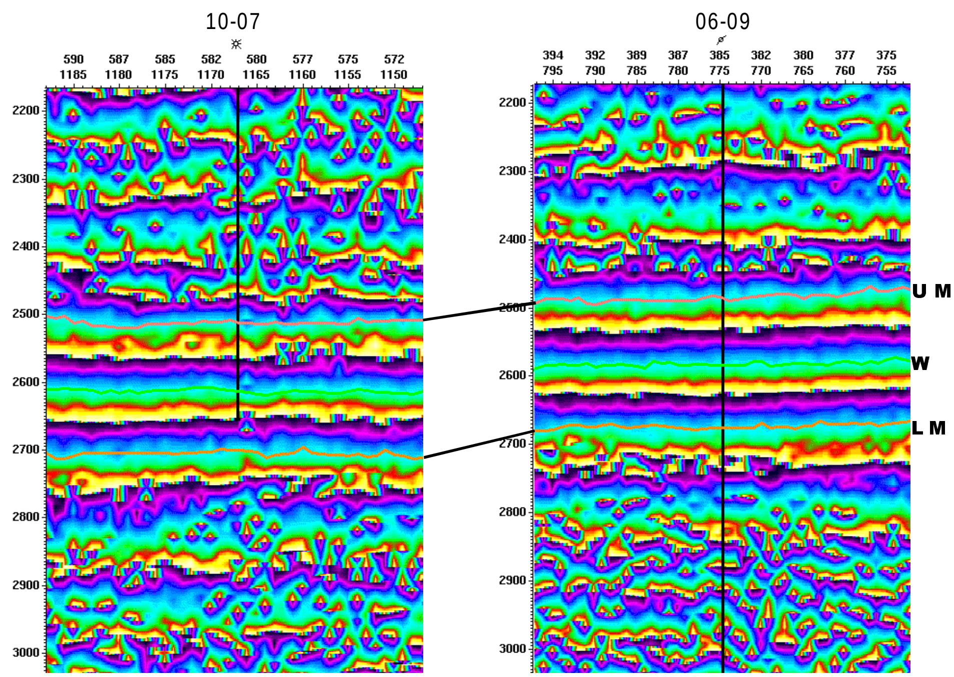

Figure 9: SH-SH instantaneous phase

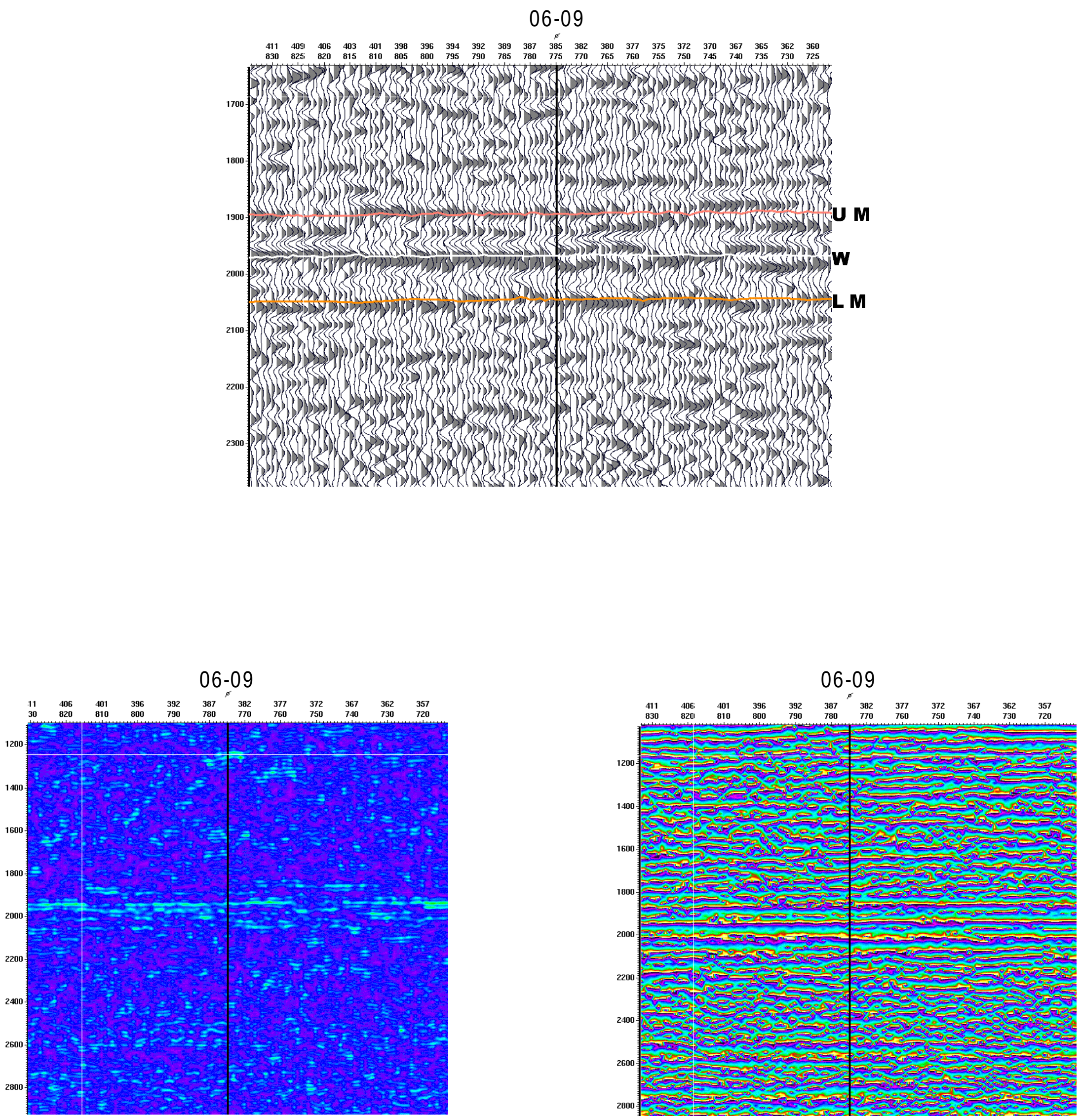

Figure 10: P-SH stack, instantaneous amplitude, and instantaneous phase.

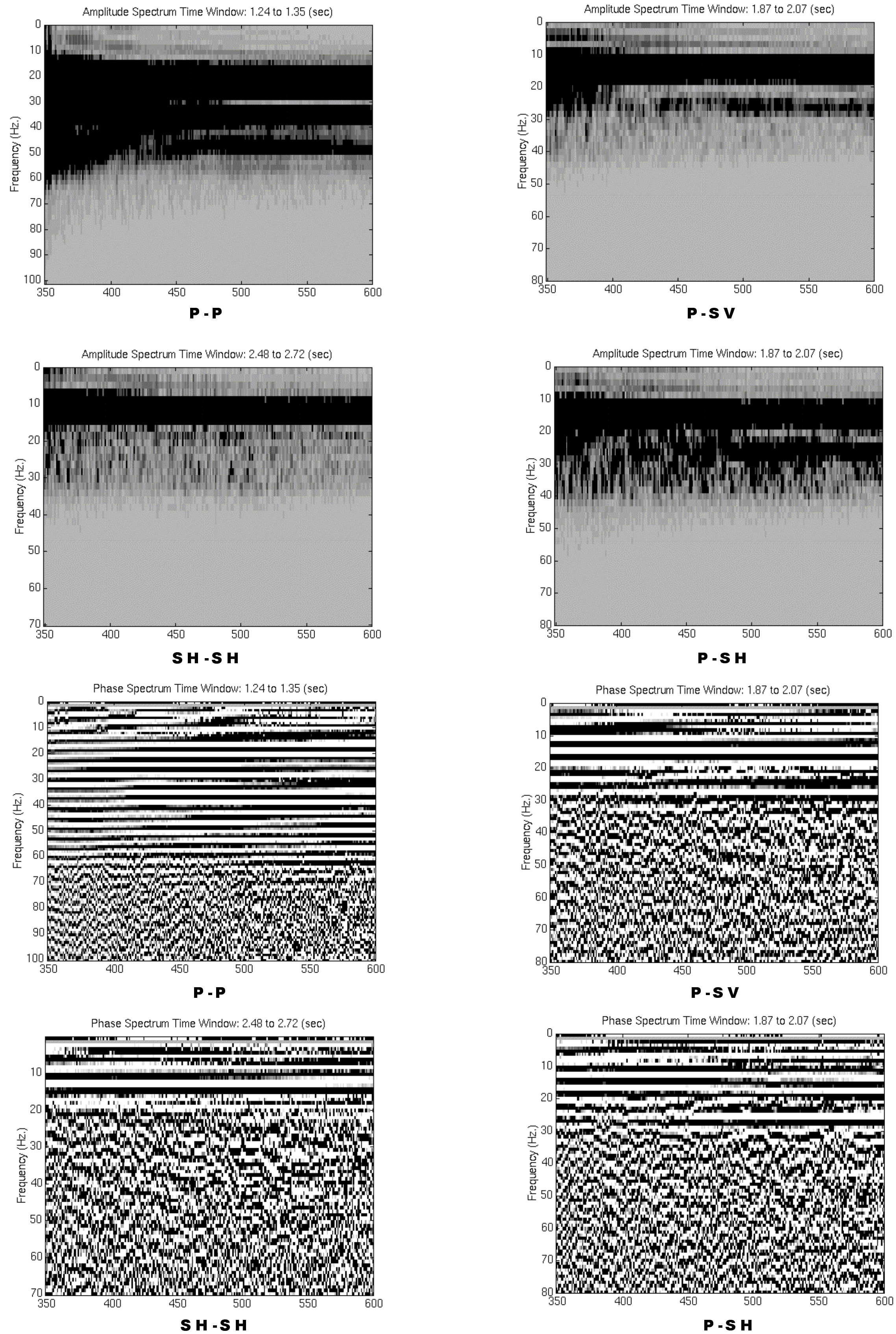

Figure 11: Frequency and phase spectra

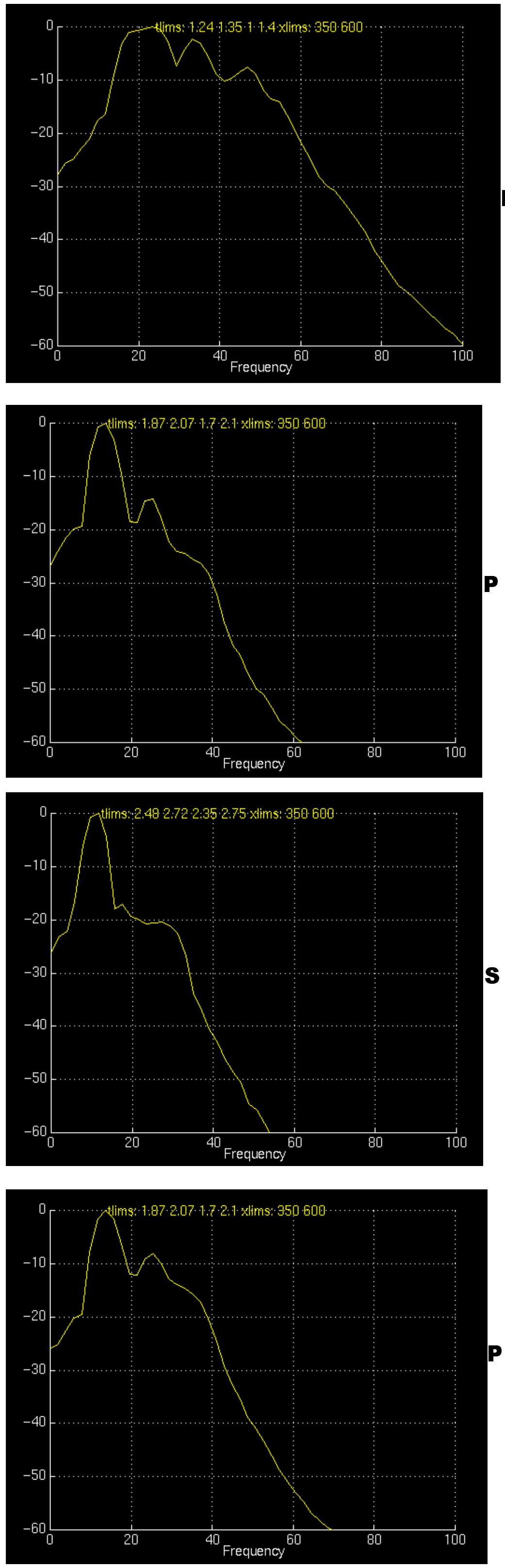

Figure 12: Average frequency spectra for the four component stacks.